Self-regulated fluctuations in the ablation of a snow patch over four decades

Koji Fujita,[1] Kuniharu Hiyama,[1,2] Hajime Iida,[3] and Yutaka Ageta[1]

Received 13 July 2009; revised 22 August 2010; accepted 27 September 2010; published 23 November 2010.

[1] We describe four decades of temporal fluctuations in the ablation of the Hamaguri-yuki snow patch in the northern Japan Alps. Annual ablation depth through the melting season shows a significant correlation with the initial depth (at the beginning of the melting season), whereas a less significant correlation is found with a temperature index that is generally believed to correlate well with ablation. The scale effect of the snow patch, which appears to modify the wind speed over the patch, has a more significant effect on snow ablation than does the radiation shadowing effect of surrounding mountains. In the case of a thinner and therefore smaller initial springtime snow patch, the speed of the local wind may be reduced over the snow surface, thereby suppressing ablation, whereas wind speed is not reduced (and ablation is not suppressed) in the case of a thicker snow patch. This self-regulating feedback means that over the past four decades, the thickness of the snow patch has fluctuated in a manner that is largely independent of summertime temperature. Our findings also suggest that the self-regulating feedback, which influences ablation, allows some small wind-drifted glaciers to survive, whereas previous studies reported enhanced accumulation at such glaciers via a similar topographic effect on wind speed and suppressed ablation via the shading effect of surrounding mountains on solar radiation.

Citation: Fujita, K., K. Hiyama, H. Iida, and Y. Ageta (2010), Self-regulated fluctuations in the ablation of a snow patch over four decades, *Water Resour. Res.*, *46*, W11541, doi:10.1029/2009WR008383.

1. Introduction

[2] Snow patches constitute a significant element of high mountain landscapes, and their temporal change has a marked effect on high-alpine runoff [*Shultz*, 1956; *Sosedov and Seversky*, 1963; *Higuchi et al.*, 1979]. Perennial snow patches generally exist below the altitude of the glaciological equilibrium line, where annual accumulation is equivalent to ablation. The formation of snow patches results from local processes of snow accumulation, the redistribution of snow due to wind and/or avalanche, and local reductions in ablation. Consequently, accumulation and ablation on snow patches cannot be described by the regional mean meteorological conditions of the free atmosphere. The stable existence of snow patches requires a long-term mass balance of zero; otherwise, the patch would become a glacier or seasonal snow cover. Because the annual mass balance of snow patches is strongly affected by year-to-year changes in seasonal weather conditions, such patches are thought to be a useful index of climate change in high mountain environments [*Watson et al.*, 1994].

[3] Despite the dependence of snow patches on year-to-year weather conditions, they can survive for many years at the same site [*Glazirin*, 1997; *Yamaguchi et al.*, 1998]. Consequently, annual variations in weather conditions are unlikely to regulate the stable existence of snow patches. To explain the survival of snow patches, previous studies have proposed hypotheses involving stabilizing feedback mechanisms, in which mass balance is inversely related to snow-patch size [*Glazirin et al.*, 2004]. The influence of the topography on wind-blown snow has been evaluated by examining the distribution of snow patches in Iceland [*Brown and Ward*, 1996], the stratigraphy of snow in Arctic Alaska [*Sturm et al.*, 2001], snow accumulation upon alpine glaciers [*Machguth et al.*, 2006], and temporal changes in the area of cirque glaciers in the Rocky Mountains [*Hoffman et al.*, 2007].

[4] Snow tends to accumulate to a greater degree upon the leeward side of topographic highs and in depressions than upon upwind slopes and convex ground, due to weakening of the local wind in the former cases [*Liston and Sturm*, 1998; *Glazirin et al.*, 2004; *Lehning et al.*, 2008; *Mott et al.*, 2008; *Raderschall et al.*, 2008; *Dadic et al.*, 2010]. On the other hand, the suppression of ablation that occurs via the shading effect of surrounding mountains has been discussed previously with respect to glacier melt [e.g., *Arnold et al.*, 1996; *Hock*, 1999; *DeBeer and Sharp*, 2009]. In addition, from a climatological perspective, a previous study reported only a minor influence on snow depth of recent warming in mountainous areas of Japan [*Yamaguchi et al.*, 2007], whereas long-term snow depth observations at lower sites facing the Japan Sea have shown a significant decrease in winter snow depth due to warming [*Ishizaka*, 2004]. A weak response of snow cover to recent warming has also been reported at high elevations in the Alps [*Marty*, 2008]. However, no previous study has sought to quantita-

[1]Graduate School of Environmental Studies, Nagoya University, Nagoya, Japan.
[2]Now at Nagoya City Hall, Naka-ku, Nagoya, Japan.
[3]Tateyama Caldera SABO Museum, Ashikuraji, Japan.

0043-1397/10/2009WR008383

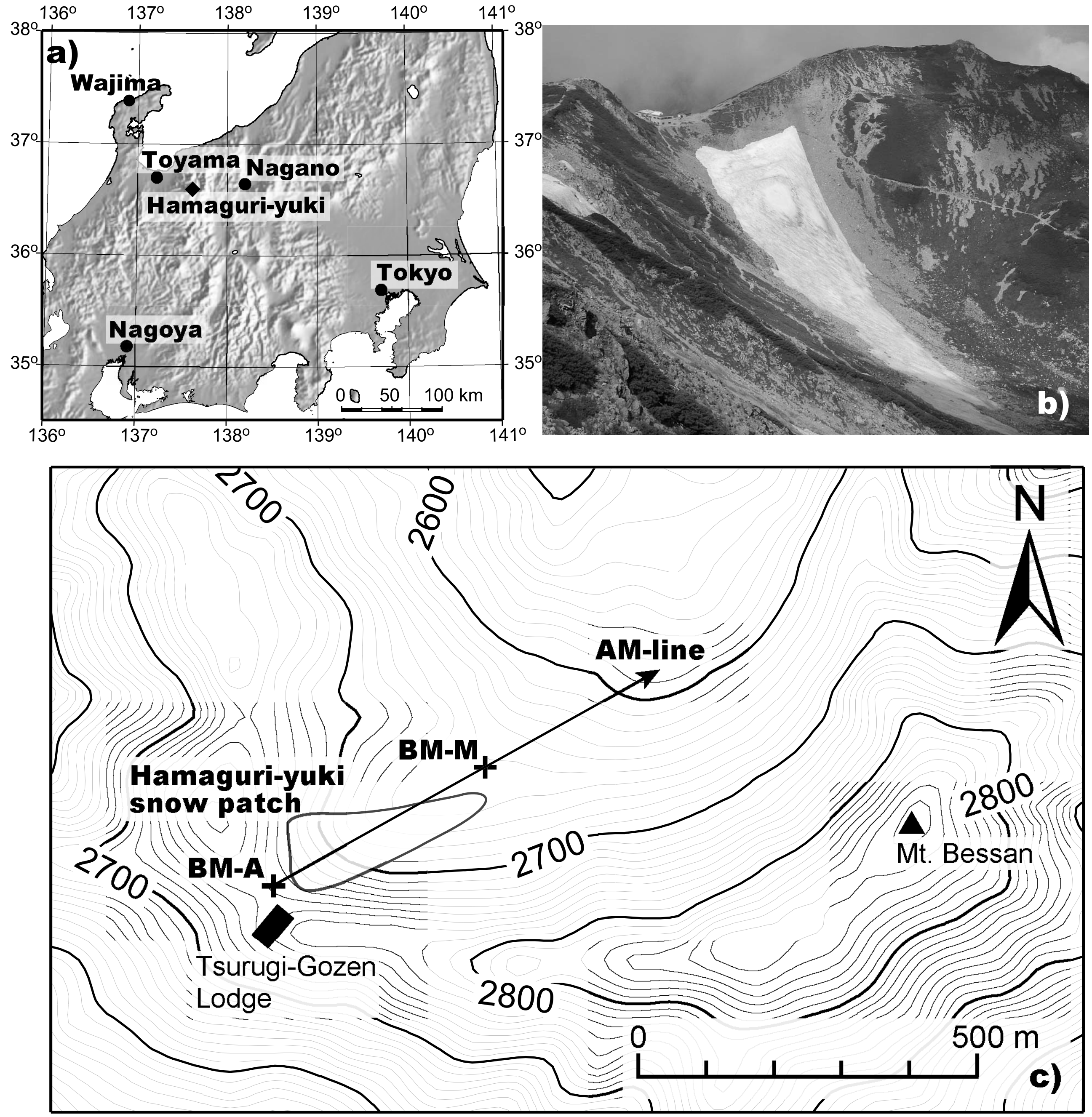

Figure 1. (a) Location map, (b) photograph, and (c) topographic map of the Hamaguri-yuki snow patch. GTOPO30 and 50 m digital elevation models published by the Geographical Survey Institute of Japan were used to construct Figures 1a and 1c, respectively. The photograph of the snow patch (Figure 1b) was taken from Mt. Bessan on 18 October 2006, the location of which is shown in Figure 1c.

tively evaluate long-term variations in the thickness of snow patches. To understand the nature of temporal fluctuations in snow depth with respect to climate at high elevations in Japan, we measured long-term fluctuations in a snow patch over the past four decades, considering the influence of the topography in mitigating ablation.

2. Study Site and Long-Term Observations

[5] The Hamaguri-yuki snow patch (see Figure 1b) is located at 2730 m above sea level (a.s.l.) in the northern Japan Alps, Central Japan (Figure 1a; 36°35.8′N, 137°36.6′E). The snow patch is formed by the accumulation of a large amount of surplus snow on the northeast facing lee slope of a mountain under a northwesterly monsoon during winter [*Higuchi et al.*, 1979]. The patch has been surveyed twice a year since 1967 [*Ohata et al.*, 1993]. A surface profile along the A-M line between benchmarks A and M (BM-A and BM-M in Figure 1c), which is set along the centerline of the valley (oriented N60°E), is surveyed each year at the beginning of the melting season (late May to early June; hereafter, spring) and again at the end (late September to

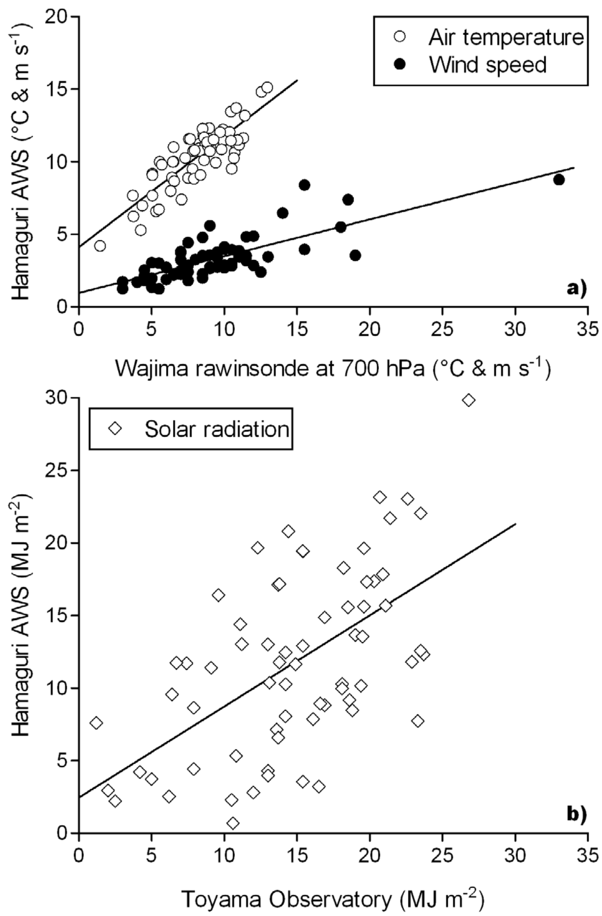

Figure 2. (a) Relationships between meteorological data at 700 hPa, as determined by rawinsonde observations at Wajima Local Meteorological Observatory (JMA), and daily air temperature (r = 0.847, $p < 0.001$) and wind speed (r = 0.777, $p < 0.001$) at the Hamaguri-yuki snow patch. (b) Relationship between daily solar radiation at the snow patch compared with that at Toyama Local Meteorological Observatory (JMA) (r = 0.581, $p < 0.001$) during the melting season of 2005.

early October; hereafter, autumn). The boundary of the patch is also measured in autumn. The surface profile along the A-M line is surveyed at 10 to 30 m horizontal intervals by tachymetry, trigonometric leveling, or theodolite with a laser distance finder. Details of past surveys and data are summarized by *Ohata et al.* [1993]. Snow depths are reported as average values over sections between 50 and 100 m points from BM-A along the A-M line, as snow has tended to survive along this section at the end of the melting season for the past 40 years. The basal profile of this section was measured when the snow patch disappeared completely in the autumn of 1998.

3. Method

[6] To evaluate the influence of the scale effect on ablation of the snow patch, we calculated the ablation depth of the patch using a heat balance model, employing estimated long-term meteorological data over the 40 year observation period.

3.1. Observations and Estimation of Meteorological Variables

[7] Because no long-term meteorological data are available near the snow patch, it is necessary to estimate meteorological variables, based on observed data from the nearest official observatories, to run the snowmelt model described below. To establish the relations between the long-term data and local variables, we observed meteorological variables (air and ground temperature, relative humidity, wind speed, wind direction, downward and upward solar radiation, and net radiation) using an automatic weather station (AWS) installed near benchmark M (BM-M in Figure 1c) during the melting season in 2005. Variables were sampled every 10 s and average values were recorded every 30 min. We use daily values in the following analysis. We compared the daily air temperature and wind speed at the snow patch with those at 700 hPa (about 3000 m a.s.l.), as obtained by rawinsonde observations (generally two measurements per day) at Wajima Local Meteorological Observatory, located 100 km northwest of the snow patch (Figure 1a), where long-term continuous observations are performed by the Japan Meteorological Agency (JMA).

[8] Both air temperature and wind speed show significant correlations (Figure 2a, r = 0.847 for air temperature and r = 0.777 for wind speed, both $p < 0.001$). Daily solar radiation can be estimated from measurements at Toyama Local Meteorological Observatory (JMA), located 40 km west-northwest of the snow patch (Figures 1a and 2b; r = 0.581, $p < 0.001$). The parameters for linear regression are summarized in Table 1. For long-term calculations, it is necessary to estimate downward long-wave radiation (R_L). This is obtainable from the downward (R_S) and reflected (R_R) short-wave radiation, net radiation (R_N), and surface temperature (T_S) observed on bare ground at the AWS site, as follows:

$$R_L = R_N - R_S + R_R + \sigma T_S^4 \quad (1)$$

where σ is the Stefan–Boltzmann constant and we assume the bare ground to behave as a blackbody. The obtained downward long-wave radiation was then compared with air temperature (Figure 3 and Table 1; r = 0.661, $p < 0.001$). Although consideration of relative humidity improves the robustness of the estimated long-wave radiation [*Fujita and Ageta*, 2000; *Fujita et al.*, 2007], we use only air temperature because long-term relative humidity data are unavailable for the snow patch. Relative humidity for turbulent heat fluxes is assumed to be constant at 87%, which was the average value of the observation over the snow patch for 2005.

[9] To convert the calculated snowmelt to ablation depth, it is necessary to know the density of the snow patch. The surface snow densities of the snow patch were measured several times during the melting seasons of 1997 and 2005, yielding values of 420–730 kg m^{-3}. We estimated monthly values of surface snow density based on observational data (measured 3–4 times per month) published in a previous study [*Nagata*, 1998] and using data from the present study (Table 2).

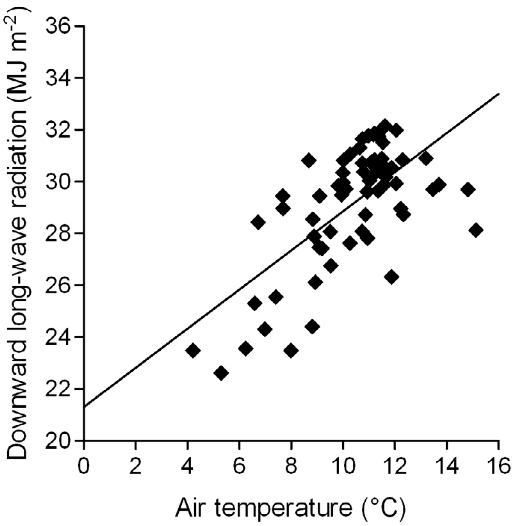

Figure 3. Air temperature plotted against downward long-wave radiation obtained by AWS in 2005 ($r = 0.661$, $p < 0.001$).

[10] The surface albedo of the snow patch, which decreases with time during the melting season [*Moribayashi et al.*, 1984; *Nagata*, 1998], is also important in estimating the absorption of solar radiation. As with the density values, we estimated monthly albedo values based on observational data collected during the melting seasons of 1997 and 2005 (measured 3–4 times per month), as published in a previous study [*Nagata*, 1998] and based on data from the present study (Table 2).

3.2. Heat Balance Over the Snow Patch

[11] Heat for snowmelt (Q_M) is calculated as

$$Q_M = R_N + Q_S + Q_L \tag{2}$$

where the sum of net radiation (R_N), and sensible (Q_S) and latent (Q_L) turbulent heat fluxes causes snowmelt over the patch. Net radiation is calculated as

$$R_N = (1 - \alpha)R_S + R_L - 315.6 \tag{3}$$

where the absorbed solar radiation at the surface is obtained from downward solar radiation (R_S) and surface albedo (α). Although downward long-wave radiation (R_L) is generally affected by air temperature, relative humidity, and cloudiness, we established a linear relation between downward long-wave radiation and air temperature, as described above. A melting surface (surface temperature of 0°C) releases upward long-wave radiation of 315.6 W m^{-2}. Q_S and Q_L are obtained by the bulk methods used for Asian glaciers [*Fujita and Ageta*, 2000; *Fujita et al.*, 2007], as follows:

$$Q_S = c_a \rho_a C u_s T_a$$
$$Q_L = l_e \rho_a C u_s \left[\frac{h_r}{100} q(T_a) - 5.08 \times 10^{-3}\right] \tag{4}$$

where c_a is the specific heat of air (J kg^{-1} K^{-1}), ρ_a is the density of air (kg m^{-3}) assuming a constant air pressure of 750 hPa at about 2700 m a.s.l., C is a bulk coefficient, and l_e is the latent heat of evaporation (2.50×10^6 J kg^{-1}). Wind speed over the snow patch (u_s) is the focus of this study and is discussed below. The saturated specific humidity (q, no dimension) of the atmosphere is obtained from air temperature (T_a, °C) and relative humidity (h_r, %). The saturated specific humidity of the melting surface is 5.08×10^{-3}. Conductive heat is negligible because the snow patch is wet during the melting season. The bulk coefficient was tuned to fit the turbulent fluxes to observational results [*Moribayashi et al.*, 1984].

Table 1. Parameters for Linear Regression Equations ($y = ax + b$)[a]

y	x	a	b	R^2
AT_h	AT_w	0.77	4.12	0.717
WS_h	WS_w	0.25	0.96	0.604
SRD_h	SRD_t	0.63	2.45	0.338
LRD_h	AT_h	0.76	21.30	0.437

[a]AT, WS, SRD, and LRD denote air temperature, wind speed, downward solar radiation, and long-wave radiation, respectively. Subscripts w, t, and h denote 700 hPa at Wajima Local Meteorological Observatory (JMA), the Toyama Local Meteorological Observatory (JMA), and the Hamaguri-yuki snow patch, respectively.

Table 2. Monthly Surface Snow Density and Surface Albedo at the Hamaguri-yuki Snow Patch Based on the Observations in 1997 [*Nagata*, 1998] and 2005 (This Study)

	Density (kg m^{-3})	Albedo
June	450	0.72
July	550	0.60
August	650	0.48
September	750	0.36

3.3. Influence of the Topography on Wind Speed

[12] We focused on the topographic effect of the snow patch on wind speed because the dominant component of heat that results in melting of the patch is turbulent fluxes [*Moribayashi et al.*, 1984]. The effect of undulations in the topography on wind speed has been investigated previously with respect to snowdrift [e.g., *Jackson and Hunt*, 1975; *Liston and Sturm*, 1998; *Lehning et al.*, 2008; *Mott et al.*, 2008; *Raderschall et al.*, 2008; *Dadic et al.*, 2010]. The results of simulations performed in these previous studies reveal that wind speed is weakened on the leeward side of topographic highs and in depressions. In particular, the topographic effect on wind is significant in steep terrain such as the Alps [*Lehning et al.*, 2008; *Raderschall et al.*, 2008]. Wind flow across the snow patch analyzed in the present study is strongly affected by its position on the leeward side of a mountain ridge (e.g., flow detachment under the prevailing wind direction from the west-south-west; Figure 4). We investigate the effect of wind speed on the ablation process, whereas previous studies have mainly focused on accumulation processes [e.g., *Jackson and Hunt*, 1975; *Liston and Sturm*, 1998; *Lehning et al.*, 2008; *Mott et al.*, 2008; *Raderschall et al.*, 2008; *Dadic et al.*, 2010].

[13] We explore here whether reduced turbulent heat flux (sensible heat) could be responsible for the observed self-regulating behavior. Snow patches are always connected to concave terrain features. These concave terrain features act increasingly as a type of bucket as the snow patch gets smaller. As the snow retreats into his bucket, it becomes decoupled from the atmosphere. Two connected processes

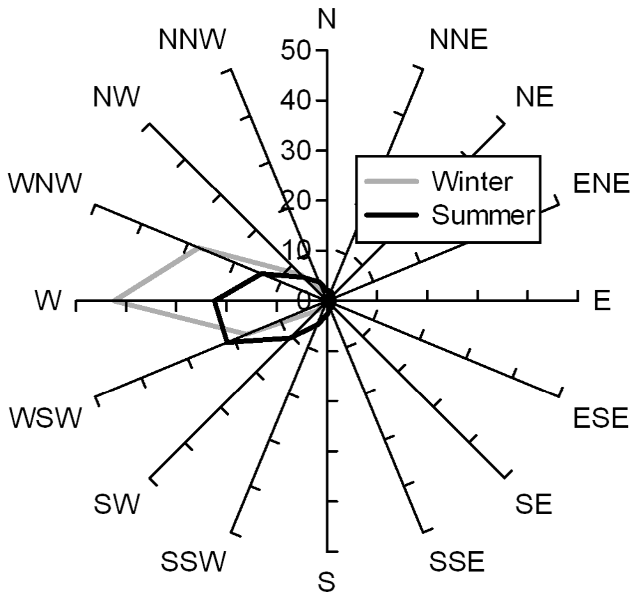

Figure 4. Prevailing wind directions in winter (December–February) and summer (June–August) for a grid including the Hamaguri-yuki snow patch. Averages at 700 hPa were obtained for the period 1968–2007 (40 years) from NCEP/NCAR reanalysis data [*Kalnay et al.*, 1996].

contribute to this decoupling: (1) the local wind speeds will be reduced due to the "bucket" terrain sheltering causing flow separation, and (2) the reduced wind speeds are facilitating thermal decoupling, where a cold air pool is able to stagnantly remain over the snow patch. Both effects are connected via a positive feedback mechanism, in which the cold air leads to a locally stably stratified boundary layer and facilitates decoupling from the airflow above and in which the reduced surface wind helps the formation of the cold air pool. Since this nonlinear response is difficult to quantify without running a fully coupled boundary layer model, we choose here to only explore the potential effect of reduced sensible heat flux via an assumed reduction of the local wind speed. We simply assume that wind speed over the snow patch (u_s) is modified by topography as follows:

$$\begin{aligned} u_s &= K u_g \\ K &= a\, d_s + b \end{aligned} \tag{5}$$

where the general wind speed (u_g), which is unaffected by topography, is modified over the snow patch. A weighting factor (K) is applied, varying linearly with the depth of the snow patch (d_s). The general wind speed is assumed to be that at the ridge upslope of the snow patch (Figure 1c). For snow depth, we used the average value between the 50 and 100 m points from BM-A along the A-M line. In the following calculation, we systematically varied the slope (a, 0.001 step) and intercept (b, 0.01 step) values for equation (5) to obtain the relation between snow patch depth and the weighting factor, and thereby calculated temporal changes in ablation depth for the four decades of the study period. For each relation between snow depth and the weighting factor, the monthly ablation depth (melted snow thickness) is obtained using the daily temperature and wind speed, monthly solar radiation, albedo, and snow density. The spring snow depth in each year is used as the initial condition for each year in the calculation. By subtracting the monthly ablation depth from the snow depth, we obtained a new snow depth, and thus a weighting factor for the following month. We performed an iterative calculation for the entire melting period based on the actual dates on which observations were undertaken each year.

4. Results and Discussion

4.1. Annual Variations in Snow Patch Depth

[14] Figure 5 shows annual variations in the spring and autumn snow depths of the snow patch since 1967, revealing large annual variability with a significant increase in spring depth ($p < 0.05$; Mann–Kendall test) and no significant trend for autumn. The average spring and autumn snow depths for the analysis period are 19.4 and 3.7 m, respectively. The standard deviation (σ) and its proportion (%) of the average value are 2.9 m and 15% for spring and 2.4 m and 65% for autumn. We define the ablation depth as the difference between the spring and autumn depths in each year. The ablation depth also shows large annual variability (σ = 2.4 m, representing 15% of the average value of 15.8 m), without any statistically significant trend.

[15] Observational studies on the snow patch have revealed a significant correlation between ablation and turbulent heat fluxes [*Moribayashi and Higuchi*, 1980; *Moribayashi et al.*, 1984], although *Ohmura* [2001] provided a different explanation of the physical basis for the temperature-based melt-index method. *Ohmura* [2001] concluded that air temperature information is transferred to the surface mainly through long-wave atmospheric radiation, which is by far the most important heat source for melting. In either case, ablation correlates with the positive degree-day sum. However, the relation between the positive degree-day sum and ablation depth, as shown in Figure 6a, shows no significant correlation ($r = 0.036$), suggesting that the regression coefficient (i.e., the degree-day factor) changes year-by-year and that change in summertime temperature has an insignificant effect on change in ablation of the snow patch.

[16] In the case of a small snow patch, it is plausibly that the surroundings (local temperature) without snow cover

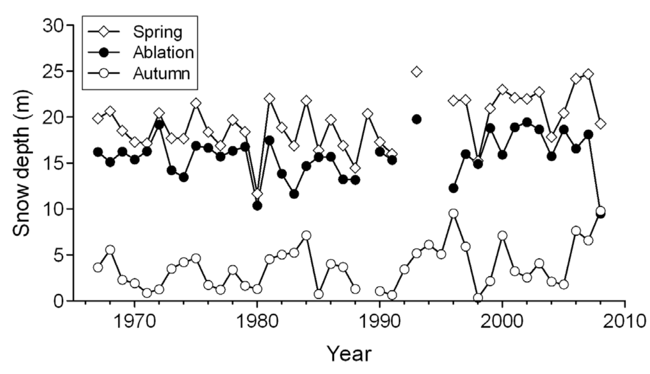

Figure 5. Fluctuations in snow depth at the Hamaguri-yuki snow patch along the A-M line at the beginning (spring) and end (autumn) of the melting season and the difference between the two (ablation) since 1967.

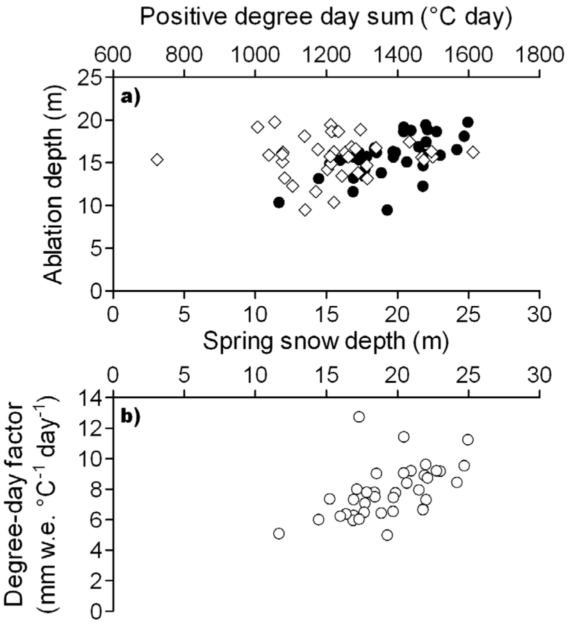

Figure 6. (a) Relations between ablation depth and positive degree-day sum (open diamonds, $r = 0.036$), and springtime snow depth (solid circles, $r = 0.590$, $p < 0.001$), and (b) relation between springtime snow depth and degree-day factor ($r = 0.534$, $p < 0.001$) for the Hamaguri-yuki snow patch.

would be warmer due to low albedo, leading to enhanced melt. Therefore, a higher degree-day factor is expected for smaller snow patches because the positive degree-day sum is estimated from the general temperature. However, the degree-day factor shows the opposite (i.e., positive) significant correlation with springtime snow depth (Figure 6b; $r = 0.534$, $p < 0.001$). This result is somewhat counterintuitive, but may reflect that these locations have geographical characteristics that protect the snow from melting beyond that represented in the degree-day analysis. However, we have no plausible physical explanation for such a relation so that an alternative mechanism should be considered. On the other hand, we found a significant positive correlation between springtime snow depth and ablation depth (Figure 6a; $r = 0.590$, $p < 0.001$). This relation indicates that a thicker springtime snow patch experiences greater melting during the succeeding summer. In other words, the snow patch is able to survive as a result of reduced melt, even in the case of thin springtime patch thickness.

4.2. Topographic Effect via Modified Wind Speed

[17] Figure 7 shows the effect on the weighting factor of parameters in the linear regression equation (equation (5)). The color scale used in Figure 7 indicates the correlation coefficient obtained between calculated and observed ablation depths. A steeper slope (a) for the equation (5) results in enhanced annual variability in ablation depth and thus yields a more significant correlation. On the other hand, improved representativeness of the calculation, which is defined as the root-mean-square error (RMSE) of the difference between calculated and observed ablation depths (solid contour lines in Figure 7), is found in the limited area around smaller intercept values (b). Although the best estimate (i.e., the smallest RMSE with a higher correlation coefficient) is found at a slope between 0.05 and 0.06 with a zero intercept, it is implausible that no wind speed should be assumed at the time when the snow patch disappeared. Because it is difficult to narrow down the best set of parameters, however, we assumed that a set of parameters (a and b) for wind reduction might be located somewhere the RMSEs are smaller than 2 m and then obtained 166 sets of parameters.

[18] Figure 8 shows a time sequence of observed and calculated ablation depths for the calculated period of 38 years. The wind-calibrated ablation depth is average of 166 set of parameters and its standard deviation is depicted with gray hatch. We also calculated the ablation depth using the general wind speed (u_g) instead of the calibrated wind speed (u_s), applying the parameters shown in Figure 7 (open black circle, slope (a) = 0 and intercept (b) = 1; thus, K = 1 at any depth). In the case of noncalibrated wind speed, we obtained a greater ablation depth (21.2 m) than that observed (15.8 m), resulting in a large RMSE of 5.56 m, and found no significant correlation (Figure 9a; $r = 0.162$). However, if the topographic effect on wind is taken into account to obtain the best estimate, as mentioned above, the difference from the observed ablation depth is relatively small (difference between average values is 0.059 m; RMSE is 1.93 m), yielding a significant correlation between the two data sets (Figure 9a; $r = 0.639$, $p < 0.001$). The difference between calibrated and noncalibrated calculations is enhanced in the case of small initial springtime snow depth (Figure 9b; $r = 0.805$, $p < 0.001$). The relatively small difference between calibrated and noncalibrated ablation depths during the most recent decade (Figure 8) is due to a relatively thick springtime snow depth in recent years (Figure 5).

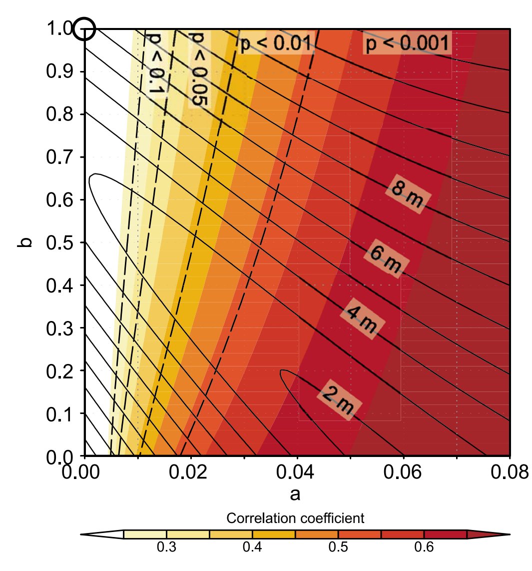

Figure 7. Effect of a linear regression equation for the weighting factor (K) on the calculated ablation depth of the Hamaguri-yuki snow patch, for the 38 year analysis period since 1967. Color contours represent the correlation coefficient between calculated and observed ablation depths; dashed lines show significance levels. Solid contour lines show the root-mean-square errors of the difference between calculated and observed ablation depths. Open black circle denotes the parameter set to obtain the weighting factors for noncalibrated result (see Figure 8).

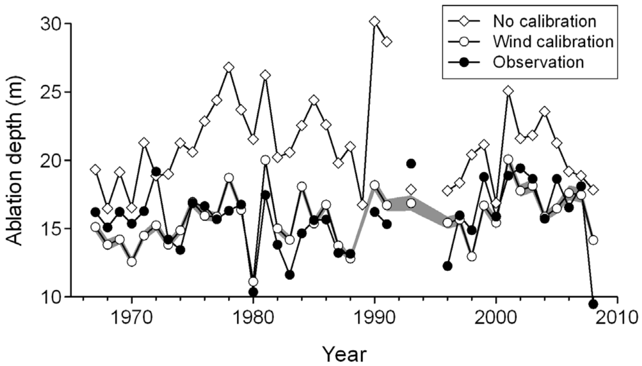

Figure 8. Observed (solid circles) and calculated (open symbols) ablation depths at the Hamaguri-yuki snow patch since 1967. The wind-calibrated results with error hatch (gray shading) are obtained from 166 sets of parameters which result in the RMSE smaller than 2 m. The set of parameters used to obtain the weighting factors for noncalibrated result are shown as open black circle in Figure 7.

[19] The above results indicate that climatic forcing on the snow patch has been damped via the influence of the topography on wind speed, which was modified by the snow patch itself. Therefore, the Hamaguri-yuki snow patch is influenced by a self-regulating feedback that controls its annual variations, thereby enabling it to survive. With a thicker initial springtime snow depth, more melt occurs, which may be caused by a smaller reduction in wind speed. In contrast, in the case of smaller initial springtime snow depth, melting may be suppressed by the weakened wind. The largest difference among the weighing factors for springtime snow depth (0.37) corresponds to a 3.0 m ablation depth if this difference persists throughout the entire melting season (duration of 90 days and assuming a snow density of 600 kg m^{-3}).

[20] The contribution of turbulent heat fluxes to snowmelt is 72% (the remaining 28% is contributed by net radiation), based on the best estimate described above, thereby supporting the proposal that the dominant component of heat for melting of the patch is turbulent fluxes [*Moribayashi et al.*, 1984]. In the case without wind calibration, the contribution of turbulent fluxes to snowmelt is more significant (79% and the remaining 21% by net radiation) because the wind modified by the scale of the snow patch has a direct (reducing) effect on turbulent heat fluxes. In turn, the initial spring snow depth is a key factor in determining how the snow patch behaves in the succeeding melting season.

4.3. Alternative Topographic Effect on Solar Radiation

[21] Previous studies have investigated the possibility that the topographic effect results in suppressed snowmelt and ice melt [e.g., *Arnold et al.*, 1996; *Hock*, 1999; *DeBeer and Sharp*, 2009]. The basic concept is that steep mountain ranges cast a shadow on the glacier and thereby limit the amount of melting. *Glazirin et al.* [2004] examined the influence of the topography on snow patch formation, concluding that a thicker snow depth receives more solar radiation than does a thinner snow depth, due to the shading effect.

[22] We examined the amount of solar radiation on the snow patch in the cases of the minimum and maximum depths of the patch, considering shading by the surrounding mountain range. The heights of the surrounding ridge, relative to the snow patch and as seen from the 75 m point from BM-A along the A-M line, were obtained from a topographic map (1:25,000) published by the Geographical Survey Institute of Japan, assuming (1) the maximum snow depth and (2) zero snow depth at the snow patch. Solar angle and aspect were calculated for the location of the snow patch, and were thus compared with the angle of inclination from the snow patch to the surrounding ridge. The maximum difference in snow-patch depth (25 m) corresponds to a difference in shading duration of 45 min in September. The 45 min of extra shading corresponds to a melt amount of 1.5 mm water equivalent (w.e.) day^{-1}, as calculated using the average solar radiation before sunset observed in 2005. Even if this largest difference continued throughout the melting season, the difference in snow depth would be 0.225 m (for a duration of 90 days and snow density of 600 kg m^{-3}). Therefore, the shading effect

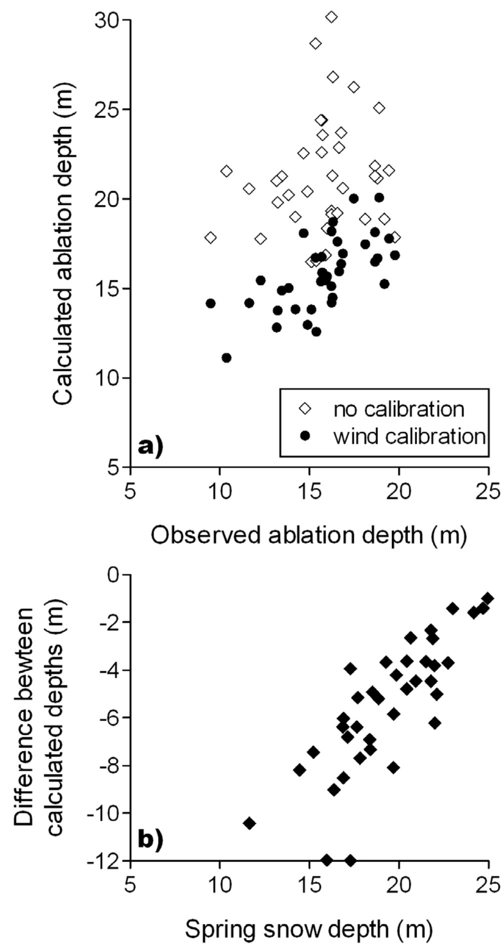

Figure 9. (a) Calculated ablation depths with wind calibration ($r = 0.639$, $p < 0.001$) and without calibration ($r = 0.162$) plotted against observed ablation depth and (b) the difference between the two ablation depths (wind calibration minus no calibration) plotted against spring snow depth ($r = 0.805$, $p < 0.001$) at the Hamaguri-yuki snow patch over the calculated period of 38 years.

proposed by *Glazirin et al.* [2004] would have a negligible influence on the relation between the springtime and ablation depths at the Hamaguri-yuki snow patch (Figure 6a).

4.4. Alternative Effect by Albedo Change

[23] Solar radiation is a major heat source for the melting of glacier ice [*Paterson*, 1994; *Fujita and Ageta*, 2000]. Consequently, the albedo of the snow-patch surface may influence ablation by controlling the absorption of solar radiation [*Fujita*, 2007, 2008]. The albedo of the snow patch decreases with time during the melting season [*Moribayashi et al.*, 1984; *Nagata*, 1998]. In particular, a sudden drop in albedo from 0.47 to 0.25 observed in August of 1997, which was 0.1 larger than the drop recorded in other studies, [*Moribayashi et al.*, 1984; this study] was thought to reflect the appearance of an older firn that had survived from the previous year [*Nagata*, 1998]. A reduction in albedo by 0.1 corresponds to a change in melt rate of 8.0 mm w.e. day^{-1}, as calculated using the average solar radiation observed in 2005, corresponding to a snow depth of 1.2 m (for a duration of 90 days and snow density of 600 kg m^{-3}). However, we emphasize that the albedo effect has an inverse influence on the relation between the initial size of the snow patch and melt amount. In other words, a thicker initial springtime depth results in less ablation depth due to the delayed appearance of older firn and the mitigation of melt, and vice versa. Therefore, the albedo effect is an implausible mechanism in explaining the relation between springtime and ablation snow depths (Figure 6a).

5. Conclusions

[24] We described temporal fluctuations in the thickness of the Hamaguri-yuki snow patch, northern Japan Alps, over the past four decades. Temporal changes in both accumulation and ablation of the snow patch show large annual variability. In particular, change in ablation depth shows a significant correlation with the initial springtime depth, whereas no correlation is found with the positive degree-day sum for each melting season, which is generally believed to be a good index of ablation. The scale effect of the snow patch, which may modify wind speed and air temperature over the patch itself as discussed above, has a greater effect on snowmelt of the patch than do the shadowing effect of the surrounding mountains and the albedo effect of old firn. In the case of a thinner initial springtime snow patch, the speed of the prevailing wind may be reduced over the snow surface in the case of the prevailing west-southwest wind (Figure 4), thereby suppressing ablation, whereas wind speed may not be reduced (and ablation is not suppressed) in the case of a thicker snow patch.

[25] Our observations and calculations suggest that annual ablation of the snow patch has fluctuated independently of summertime temperature over the past four decades, whereas snowmelt correlated significantly with air temperature on a seasonal time scale (snowmelt increased linearly with that of positive degree-day sum within a year [*Moribayashi et al.*, 1984]). In other words, the influence of variability in summertime temperature has been weakened by the topographic effect on wind speed over the snow patch, which was determined by the patch itself.

[26] *Glazirin et al.* [2004] reported that wintertime accumulation is strongly correlated with snow-patch size in the preceding autumn, via the mechanism of wind redistribution over the snow patch. A smaller snow patch in autumn enables greater accumulation, and vice versa. The results of studies on ablation (the present study) and accumulation [*Glazirin et al.*, 2004] may reveal the self-regulated nature of fluctuations in the thickness of the Hamaguri-yuki snow patch, whereby climatic influence is damped by a negative feedback with snow-patch size. It has been well verified that some small glaciers tend to fluctuate in mass balance independently of temperature, due to topographic effects on accumulation via modification of the wind field and on ablation via shading [*Kuhn*, 1995; *Machguth et al.*, 2006; *Hoffman et al.*, 2007; *Mott et al.*, 2008; *Dadic et al.*, 2010]. Our study revealed an additional topographic effect on ablation via modification of the wind field. The magnitude of this effect is determined by the size of the snow patch or glacier.

[27] The present results suggest that the self-regulating mechanism (of snow-patch size) that operates during the summertime melting season also may allow small glaciers to survive, despite the fact that glacial recession is generally thought to be a characteristic feature of global warming.

[28] **Acknowledgments.** We are deeply indebted to the staff at Tsurugigozen Lodge for their kind logistical support during long-term field surveys, and we acknowledge the many people involved in the surveys. We thank M. Lehning, R. Dadic, K. Nishimura, and two anonymous reviewers for their thoughtful comments. This research was supported by a Grant-in-Aid for Scientific Research (19253001) from MEXT, Japan.

References

Arnold, N. S., I. C. Willis, M. J. Sharp, K. S. Richards, and W. J. Lawson (1996), A distributed surface energy-balance model for a small valley glacier: I. Development and testing for Haut Glacier d'Arolla, Valais, Switzerland, *J. Glaciol.*, *42*, 77–89.

Brown, I., and R. Ward (1996), The influence of topography on snowpatch distribution in southern Iceland: A new hypothesis for glacier formation?, *Geogr. Ann., Ser. A*, *78*, 197–207, doi:10.2307/521040.

Dadic, R., R. Mott, M. Lehning, and P. Burlando (2010), Wind influence on snow depth distribution and accumulation over glaciers, *J. Geophys. Res.*, *115*, F01012, doi:10.1029/2009JF001261.

DeBeer, C. M., and M. J. Sharp (2009), Topographic influences on recent changes of very small glaciers in the Monashee Mountains, British Columbia, Canada, *J. Glaciol.*, *55*, 691–700, doi:10.3189/002214309789470851.

Fujita, K. (2007), Effect of dust event timing on glacier runoff: Sensitivity analysis for a Tibetan glacier, *Hydrol. Processes*, *21*, 2892–2896, doi:10.1002/hyp.6504.

Fujita, K. (2008), Effect of precipitation seasonality on climatic sensitivity of glacier mass balance, *Earth Planet. Sci. Lett.*, *276*, 14–19, doi:10.1016/j.epsl.2008.08.028.

Fujita, K., and Y. Ageta (2000), Effect of summer accumulation on glacier mass balance on the Tibetan Plateau revealed by mass-balance model, *J. Glaciol.*, *46*, 244–252, doi:10.3189/172756500781832945.

Fujita, K., T. Ohta, and Y. Ageta (2007), Characteristics and climatic sensitivities of runoff from a cold-type glacier on the Tibetan Plateau, *Hydrol. Processes*, *21*, 2882–2891, doi:10.1002/hyp.6505.

Glazirin, G. E. (1997), Regime of existence of old snow patches—Almost glaciers, in *34 Selected Papers on Main Ideas of the Soviet Glaciology, 1940s–1980s*, edited by V. M. Kotlyakov, pp. 314–321, Glaciol. Assoc., Moscow.

Glazirin, G. E., Y. Kodama, and T. Ohata (2004), Stability of drifting snow-type perennial snow patches, *Bull. Glaciol. Res.*, *21*, 1–8.

Higuchi, K., T. Ohata, and O. Watanabe (1979), Regional characteristics of snow patches in Japan 2: Size variation of perennial snow patch "Hamaguri-yuki" in Tsurugisawa cirque (in Japanese with English abstract), *Seppyo*, *41*, 77–89.

Hock, R. (1999), A distributed temperature-index ice- and snowmelt model including potential direct solar radiation, *J. Glaciol.*, *45*, 101–111.

Hoffman, M. J., A. G. Fountain, and J. M. Achuff (2007), 20th-century variations in area of cirque glaciers and glacierets, Rocky Mountain National Park, Rocky Mountains, Colorado, USA, *Ann. Glaciol.*, *46*, 349–354, doi:10.3189/172756407782871233.

Ishizaka, M. (2004), Climatic response of snow depth to recent warmer winter seasons in heavy-snowfall areas in Japan, *Ann. Glaciol.*, *38*, 299–304, doi:10.3189/172756404781815248.

Jackson, P. S., and J. C. R. Hunt (1975), Turbulent flow over a low hill, *Q. J. R. Meteorol. Soc.*, *101*, 929–955, doi:10.1002/qj.49710143015.

Kalnay, E., et al. (1996), The NCEP/NCAR 40-year reanalysis project, *Bull. Am. Meteorol. Soc.*, *77*, 437–471, doi:10.1175/1520-0477(1996)077<0437:TNYRP>2.0.CO;2.

Kuhn, M. (1995), The mass balance of very small glaciers, *Z. Gletscherkd. Glazialgeol.*, *31*, 171–179.

Lehning, M., H. Löwe, M. Ryser, and N. Raderschall (2008), Inhomogeneous precipitation distribution and snow transport in steep terrain, *Water Resour. Res.*, *44*, W07404, doi:10.1029/2007WR006545.

Liston, G., and M. Sturm (1998), A snow-transport model for complex terrain, *J. Glaciol.*, *44*, 498–516.

Machguth, H., O. Eisen, F. Paul, and M. Hoelzle (2006), Strong spatial variability of snow accumulation with helicopter-borne GPR on two adjacent Alpine glaciers, *Geophys. Res. Lett.*, *33*, L13503, doi:10.1029/2006GL026576.

Marty, C. (2008), Regime shift of snow days in Switzerland, *Geophys. Res. Lett.*, *35*, L12501, doi:10.1029/2008GL033998.

Moribayashi, S., and K. Higuchi (1980), Study of perennial snow patch in Tsurugisawa (2), Summer climate and snow melt processes in Tsurugisawa cirque (in Japanese with English abstract), *Seppyo*, *42*, 119–146.

Moribayashi, S., K. Higuchi, and T. Ohata (1984), Study of perennial snow patch in Tsurugisawa (3) Heat balance of snow surface (in Japanese with English abstract), *Seppyo*, *46*, 11–18.

Mott, R., F. Faure, M. Lehning, H. Löwe, B. Hynek, G. Michlmayer, A. Prokop, and W. Schöner (2008), Simulation of seasonal snow-cover distribution for glacierized sites on Sonnblick, Austria, with the Alpine3D model, *Ann. Glaciol.*, *49*, 155–160, doi:10.3189/172756408787814924.

Nagata, M. (1998), Study on size, ablation rate and distribution variations of Hamaguri-yuki, perennial snow patch in Northern Japan Alps (in Japanese), MS thesis, 32 pp., Nagoya Univ., Nagoya, Japan.

Ohata, T., H. Yabuki, K. Higuchi, O. Watanabe, S. Takenaka, H. Iida, and H. Takahara (1993), Variation of perennial snow patch "Hamaguri-yuki" from 1967 to 1991, *Res. Rep. Inst. Hydrospheric Atmos. Sci. 1*, 43 pp., Inst. for Hydrospheric Atmos. Sci., Nagoya Univ., Nagoya, Japan.

Ohmura, A. (2001), Physical basis for the temperature-based melt-index method, *J. Appl. Meteorol.*, *40*, 753–761, doi:10.1175/1520-0450(2001)040<0753:PBFTTB>2.0.CO;2.

Paterson, W. S. B. (1994), *The Physics of Glaciers*, 3rd ed., 480 pp., Pergamon, New York.

Raderschall, N., M. Lehning, and C. Schär (2008), Fine-scale modeling of the boundary layer wind field over steep topography, *Water Resour. Res.*, *44*, W09425, doi:10.1029/2007WR006544.

Shultz, V. L. (1956), *Thawing of Snow Patches in Mountains of Central Asia* (in Russian), 351 pp., Acad. of Sci. of Uzbekistan, Tashkent, U.S.S.R.

Sosedov, I. S., and I. V. Seversky (1963), On the role of avalanche snow patches in the feed of mountain rivers(in Russian), in *Problems of Hydrology of Kazakhstan, Alma-Ata*, pp. 17–33, Acad. of Sci. of Kazakhstan, Alma-Ata, U.S.S.R.

Sturm, M., G. E. Liston, C. S. Benson, and J. Holmgren (2001), Characteristics and growth of a snowdrift in Arctic Alaska, U.S.A., *Arct. Antarct. Alp. Res.*, *33*, 319–329, doi:10.2307/1552239.

Watson, A., R. W. Davison, and D. D. French (1994), Summer snow patches and climate in northeast Scotland, U.K., *Arct. Alp. Res.*, *26*, 141–151, doi:10.2307/1551777.

Yamaguchi, S., T. Shiraiwa, and R. Naruse (1998), Recent variations in mass balance of the Hisago snow patch on the Daisetsu Mountains (in Japanese with English abstract), *Seppyo*, *60*, 279–287.

Yamaguchi, S., O. Abe, S. Nakai, and A. Sato (2007), Recent snow cover fluctuations in the mountainous areas of Japan, in *Glacier Mass Balance Changes and Meltwater Discharge*, *IAHS Publ.*, *318*, 116–125.

Y. Ageta and K. Fujita, Graduate School of Environmental Studies, Nagoya University, Furo-cho, Chikusa-ku, Nagoya 464-8601, Japan. (cozy@nagoya-u.jp)

K. Hiyama, Nagoya City Hall, Sannomaru 3-1-1, Naka-ku, Nagoya, Aichi 460-0001, Japan.

H. Iida, Tateyama Caldera SABO Museum, Ashikuraji, Toyama 930-1450, Japan.